

# High Magnetic Fields in Semiconductor Nanostructures: Spin Effects in Single InAs Quantum Dots

U. Zeitler<sup>1</sup>, I. Hapke-Wurst<sup>1</sup>, D. Sarkar<sup>1</sup>, R.J. Haug<sup>1</sup>, H. Frahm<sup>2</sup>, K. Pierz<sup>3</sup>, and A.G.M. Jansen<sup>4</sup>

<sup>1</sup> Institut für Festkörperphysik, Universität Hannover, Appelstraße 2, 30167 Hannover, Germany

<sup>2</sup> Institut für Theoretische Physik, Universität Hannover, Appelstraße 2, 30167 Hannover, Germany

<sup>3</sup> Physikalisch-Technische Bundesanstalt Braunschweig, Bundesallee 100, 38116 Braunschweig, Germany

<sup>4</sup> Grenoble High Magnetic Field Laboratory, MPIF- CNRS, B.P. 166, 38042 Grenoble Cedex 09, France

**Abstract.** We present a prominent example how the influence of high magnetic fields can lead to spectacular field induced effects in a semiconductor nanostructure. We observe current steps in the  $I$ - $V$  characteristics of a GaAs-AlAs tunnelling structure with self-assembled InAs quantum dots embedded in the AlAs barrier. The steps originate from resonant tunnelling through individual InAs quantum dots. In a magnetic field the Zeeman splitting of the quantized dot states leads to a splitting of each current step in two. The Landé factor deduced from these measurements is in the range  $g = 0.6 \dots 1.5$  depending on the size of the dot and the orientation of the magnetic field. In high magnetic fields ( $B > 20$  T) the current steps evolve into extremely enhanced peaks. The effect observed is explained by a field induced Fermi-edge singularity caused by the Coulomb interaction between the tunnelling electron on the quantum dot and the partly spin-polarized Fermi sea in the Landau quantized three-dimensional emitter.

Over the last years several groups succeeded in performing single-electron tunnelling experiments through self-assembled InAs quantum dots (QDs) [1,2,3,4]. When a magnetic field is applied the spin degeneracy of the quantized energy states in an InAs QD is lifted and it is possible to resolve distinct spin states at low temperatures [5,6].

In this work we present our recent results on magneto-tunnelling experiments through self-assembled InAs QDs. We will show that we can deduce the Landé factor of a single InAs quantum dot and will analyse its dependence on the dot size and on the direction of the magnetic field applied [7,8]. In high magnetic fields ( $B > 20$  T) we find strong singularities in the resonant tunnelling through an individual InAs QD [6]. They will be explained with a theoretical model considering the electrostatic potential experienced by the emitter electrons around the Fermi edge due to the charged QD. We will show that the partial spin polarization of the Landau quantized three-dimensional

emitter causes extreme values of the edge exponent  $\gamma > 0.5$  not observed until present and going far beyond the standard theory valid for  $\gamma \ll 1$  [9].

## 1 Sample Preparation

Our samples are single barrier GaAs-AlAs-GaAs tunnelling structures with three-dimensional highly doped GaAs electrodes and self-assembled InAs QDs embedded in the middle of the AlAs barrier.

For the bottom GaAs electrode first a  $1\ \mu\text{m}$  highly doped GaAs (electron concentration  $n^+ = 2 \times 10^{24}\ \text{m}^{-3}$ ) is grown on a  $n^+$ -doped GaAs substrate at a substrate temperature of  $600^\circ\text{C}$ . This layer is followed by  $10\ \text{nm}$   $n$ -doped GaAs ( $n = 10^{23}\ \text{m}^{-3}$ ),  $10\ \text{nm}$   $n^-$ -doped GaAs ( $n^- = 10^{22}\ \text{m}^{-3}$ ) and a  $15\ \text{nm}$  nominally undoped GaAs spacer layer. The doping sequence leads to the formation of a three-dimensional electron system up to the AlAs barrier with an electron concentration  $n_e \approx 10^{23}\ \text{m}^{-3}$  at the GaAs-AlAs interface.

On top of the bottom electrode we deposit the first  $5\ \text{nm}$  of the AlAs barrier. Subsequently, the growth is interrupted and the substrate temperature is ramped down to  $520^\circ\text{C}$ . Then  $1.8$  monolayers of InAs are deposited directly onto the AlAs. Due to the strong lattice mismatch between AlAs and InAs self-assembled InAs QDs form. The dots are covered by another  $5\ \text{nm}$  AlAs and a top GaAs electrode is grown symmetrically to the bottom one.

Electric contacts are realized by annealing AuGeNi into the electrodes. At the same time, the metallic top contacts serve as an etch mask for the structuring of macroscopic tunnelling diodes with a pillar diameter of  $40 - 100\ \mu\text{m}$  containing about  $10^6 - 10^7$  InAs QDs.

To characterize the geometric properties of the InAs QDs we have produced reference samples where the growth of the structures was interrupted directly after deposition of the InAs. Additionally, we have grown uncovered InAs QDs directly on GaAs. The geometric properties of these uncovered InAs QDs can be visualized with an atomic force microscope, the results are shown in Fig. 1 [4]. The QDs forming on AlAs are considerably smaller compared to dots grown on GaAs under identical growth condition. Moreover, whereas the dot size on GaAs does not depend on the InAs coverage, it increases with coverage when the dots are grown on AlAs (not shown). In other words, the dot density for InAs dots grown on GaAs increases with increasing InAs coverage whereas it remains approximately constant for InAs QDs on AlAs. We assign this behaviour, as well as the relatively small dot size of InAs QDs on AlAs, to a reduced In diffusion on the rough AlAs surface which leads to a nucleation of QDs at positions only depending on the surface morphology.

The structural properties of the dots do not change considerably when they are covered by AlAs. This fact is visualized in Fig. 1(a) where we show a transmission electron micrograph of a complete sample with InAs dots

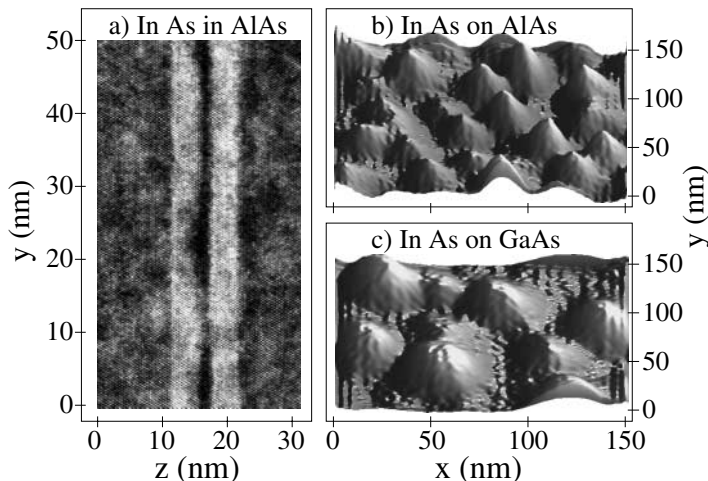


**Fig. 1.** Transmission electron micrograph of InAs dots embedded in a GaAs-AlAs-GaAs tunnelling device (a). For comparison, atomic force micrographs of uncovered reference samples are shown on the right panels with InAs quantum dots grown on GaAs (b) and on AlAs (c). (Figure taken from Ref. [4].)

embedded inside an AlAs barrier. For the samples used in our experiments the dots have a lateral diameter of 10-15 nm and a height of 3-4 nm.

## 2 Resonant Tunnelling

A current-voltage ( $I$ - $V$ ) characteristics of a typical tunnelling device containing self-assembled InAs QDs is shown in Fig. 2. For both bias directions we observed steps in the  $I$ - $V$  curve which we attribute to resonant tunnelling through the InAs QDs [4,6]. For zero bias, all quantized states of the InAs QDs are situated above the Fermi energy of the emitter,  $E_F^{em}$ . When a finite bias voltage  $V$  is applied they start moving down energetically with respect to  $E_F^{em}$ . As shown in the schematic band diagram in Fig. 2 a step occurs whenever a dot state is aligned with  $E_F^{em}$ . From the magnetic field dependence of the onset voltages of the current steps we conclude that they can be identified with resonant tunnelling through the ground states of different InAs QDs.

Due to the finite height of the InAs QDs the bottom AlAs barrier is effectively thicker compared to the top barrier, see Fig. 1(c). As a consequence, the tunnelling current is largely determined by the transmission of the bottom AlAs barrier. For positive bias electrons tunnel through this barrier first and leave the dot nearly instantaneously through the top barrier, leaving the dot nearly always empty. In this single-electron tunnelling direction it is possible to access different quantized energy levels of an InAs QD and to probe the

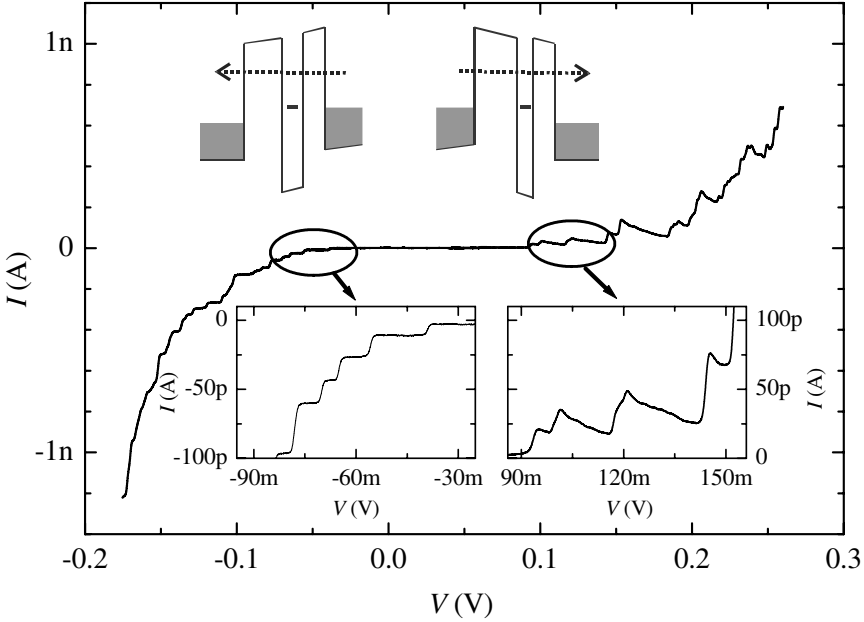


**Fig. 2.** Typical  $I$ - $V$  characteristics of a GaAs-AlAs-GaAs tunnelling diode with embedded InAs QDs measured at  $T = 0.35$  K. The top inset shows schematically the band structure for the two bias polarities. The bottom insets represent magnifications of the  $I$ - $V$  curve for negative and positive bias

electrons in the emitter with the QD, see e.g. [10]. In contrast, for negative bias the tunnelling electrons are kept mostly in the dot and Coulomb charging effects become important. For this charging direction interactions with the emitter are negligible in the tunnelling current through the dot.

### 3 Zeeman Splitting

When applying a magnetic field the current steps originating from tunnelling through InAs QDs split up into two, see Fig. 3(a). This is due to the Zeeman splitting  $\Delta E_Z$  of the quantized dot state as sketched in Fig. 3(c). A first current step occurs when the spin-down state of the dot is aligned with  $E_F^{em}$ , the second step is then due to the resonance of the spin-up level with  $E_F^{em}$ . The splitting between the two steps is given by  $\Delta V = g\mu_B B/e\alpha$  where  $g$  is the effective Landé factor of the InAs QD,  $\mu_B$  is the Bohr magneton and  $\alpha$  is a lever factor defined as the ratio of the voltage drop between the emitter and the dot and the total voltage applied. It is derived from the temperature dependence of the width of a current step at zero magnetic field caused by the thermal smearing of the Fermi edge in the emitter. Using  $\alpha = 0.34$  for

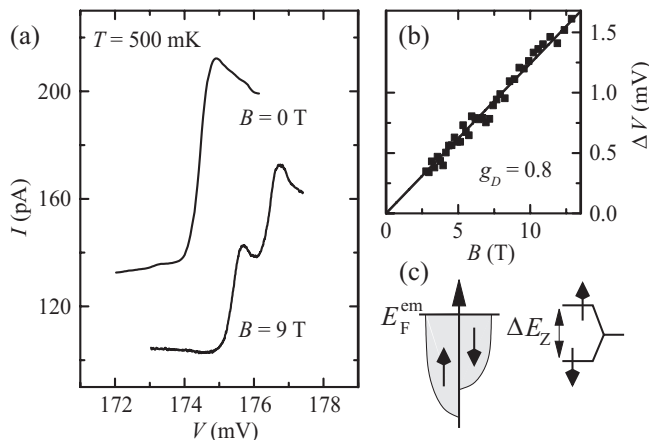


**Fig. 3.** (a) Zeeman splitting of the ground state in an InAs quantum dot visualized as the splitting of a current step observed at  $B = 0$  into two steps at  $B = 9$  T. (b) Voltage difference of the two spin-split current steps as a function of magnetic field. The line shows a linear fit corresponding to a Landé factor  $g = 0.8$ . (c) Schematic energy diagram of the emitter and an InAs QD in a magnetic field

the specific dot shown in Fig. 3 we extract  $g = 0.8$  from a linear fit of  $\Delta V$  as a function of  $B$ , see Fig. 3(b).

As sketched in Fig. 3(c) we propose in agreement with other experiments [5] that the sign of  $g$  is positive, i.e. the spin-down state is energetically situated below the spin-up state. In contrast, due to the negative  $g$ -factor in GaAs, the spin-down electrons in the emitter are energetically positioned above the spin up-electrons making the spin-up orientation the majority spin in high magnetic fields.

The fact that  $g$  for InAs QDs is positive can be deduced from the observation that the height of the first step associated with the energetically lower lying state in the dot increases with increasing temperature in high magnetic fields which is due a thermally induced higher occupation of the minority spin in the GaAs emitter with a negative  $g$ -factor [6].

We have measured the  $g$ -factor of numerous other InAs QDs [13], the results are compiled in Fig. 4. As can be clearly seen in the figure,  $g$  systematically increases with increasing onset voltage  $V_S$  of the corresponding current step. This hints to a systematically larger  $g$ -factor for smaller dots with a higher ground state energy. The absolute value of  $g$  as well as its dependence on the dot size can be explained qualitatively in the framework of a simple 3-band  $k$ - $p$  model [11]. Here the Landé factor is given as

$$g = g_0 \left[ 1 - \frac{P^2}{3} \left( \frac{1}{E_g} - \frac{1}{E_g + \Delta_0} \right) \right] \quad (1)$$

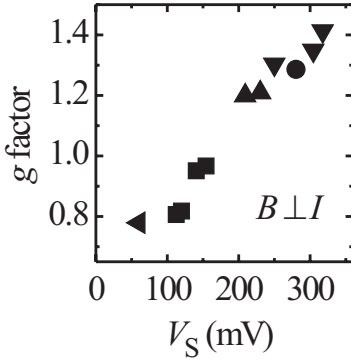


**Fig. 4.** Landé factor as a function of the onset voltage. For increasing onset voltages the corresponding dot size is decreasing

with  $g_0 = 2$ .  $P^2 = 22$  eV is the interband matrix element for InAs and  $\Delta_0 = 0.38$  eV is the valence-band spin-orbit splitting for InAs. In reality a small alloying of AlAs into the InAs QDs has to be considered which slightly reduced  $P^2$  and  $\Delta_0$  by about 10%. This makes it reasonable to use  $P^2 \approx 20$  eV and  $\Delta_0 \approx 0.34$  eV for the further calculations.

The energy gap  $E_g$  between valence band electrons and conduction band holes in the InAs QDs can be determined from photoluminescence measurements to be in the range  $E_g = 1.64$  eV - 1.76 eV [12]. Within this simple model this yields theoretically expected  $g$ -factors varying from 0.6 to 0.8 for the dots with gaps in this range, in reasonable agreement with the experimentally measured values.

The Landé factor of an InAs quantum does not only depend on the dot size but also on the orientation of the magnetic field. This can be expressed in a simple way phenomenologically as

$$g(\vartheta, \varphi) = \sqrt{(g_{[0\bar{1}\bar{1}]}^2 \sin^2 \varphi + g_{[0\bar{1}\bar{1}]}^2 \cos^2 \varphi) \cos^2 \vartheta + g_{[100]}^2 \sin^2 \vartheta}. \quad (2)$$

The angles  $\vartheta$  and  $\varphi$  are defined in the top panels of Fig. 5. Indeed, as shown in Fig. 5 the experimentally measured  $g$ -factor shows the expected behaviour, a finding also confirmed by systematic measurements on more dots [13].

The major effect of the  $g$ -factor anisotropy is observed when the magnetic field is tilted from the growth direction [100] into the  $[0\bar{1}\bar{1}]$  direction inside the growth plane, see Fig. 5(a) [7]. The measured  $g$ -factors  $g_{[0\bar{1}\bar{1}]}$  and  $g_{[100]}$  differ by about 30%. We assign this to a larger influence of size quantization effects when the magnetic field is perpendicular to the direction of the strongest confinement. Such a  $g$ -factor anisotropy was also predicted theoretically for non-spherical systems [14].

Astonishingly also a small but measurable  $g$ -factor anisotropy is observed when  $B$  is tilted inside the growth plane, with  $g_{[0\bar{1}\bar{1}]}$  being about 10% larger than  $g_{[0\bar{1}1]}$ , see Fig. 5(b) [8]. This observation hints to a slightly elongated base of the InAs QDs along the  $[0\bar{1}\bar{1}]$  direction leading to a larger influence

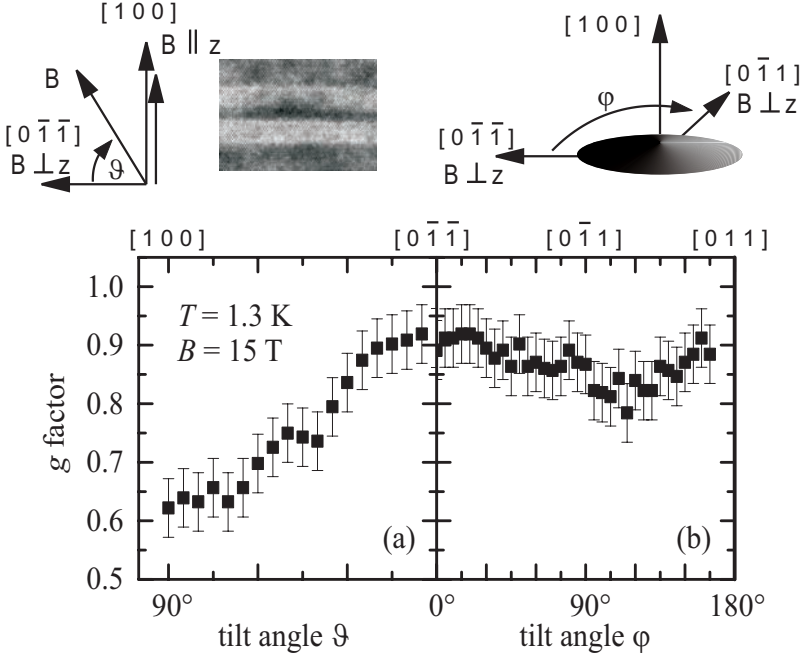


**Fig. 5.** Landé factor of one specific InAs QD as a function of the magnetic field direction. In (a) the field is tilted from the growth direction  $z$  into the growth plane  $x$ - $y$ . In (b)  $B$  is turned by  $180^\circ$  inside the growth plane. The top panels show schematically the orientation of the magnetic field for the two configurations (a) and (b)

of size quantization effects on  $g$  when the magnetic field points along this direction.

## 4 Fermi-Edge Singularities

For moderate magnetic fields ( $B < 10$  T, Fig. 3) the two current steps assigned to the tunnelling through a spin-split InAs QD state are comparable in height to half the step height at zero field. In large magnetic fields, however, they start to evolve into strongly enhanced peaks with a peak amplitude of more than one magnitude larger than the zero-field step height, see Fig. 6. The peaks are particularly pronounced for the spin orientation corresponding to the majority spin in the GaAs emitter.

The shape of these current peaks is characterized by a sharp ascent, with a width only limited by thermal broadening, and a moderate decrease towards higher voltages. The decrease of the current for  $V > V_S$  can be described

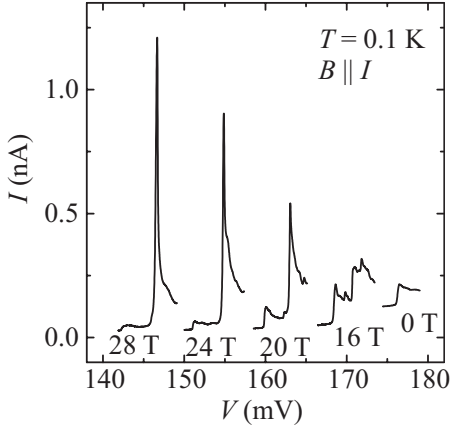


**Fig. 6.**  $I$ - $V$  characteristics of a current step at  $T \approx 0.1$  K for magnetic fields up to 28 T

within the framework of a Fermi-edge singularity (FES) [9],  $I \propto (V - V_S)^{-\gamma}$ , where  $V_S$  here is the voltage at the maximum peak current and  $\gamma$  is the edge exponent of the FES. The edge exponents  $\gamma$  extracted from the shape of the current peaks as a function of magnetic field are plotted in Fig. 7 for both spin directions.

An alternative method to determine  $\gamma$  uses temperature dependent measurements of the peak height of the FES. Here, the peak current  $I_0$  scales as  $I_0 \propto T^{-\gamma}$  [15]. The experimentally measured  $\gamma$  using this method for the majority spin are also shown in Fig. 7. It is not possible to extract the edge exponent for the minority spin directly from temperature dependent experiments. At high magnetic fields the observed increase of the current with increasing temperature is mainly caused by an additional thermal population of the minority spin in the emitter.

In order to understand the observed singularities quantitatively we have developed a theoretical model, details can be found in Refs. [6,13]. The key ingredients are the Landau quantization of the three-dimensional conduction electrons in the emitter and the Coulomb interaction between these electrons and the InAs quantum dot. In high magnetic fields, typically  $B > 6$  T for our samples, all electrons are in the lowest Landau level. We observe the strongest singularities when the field is applied along the current direction. In this case the Landau quantized electrons can be described by quasi one-dimensional channels with momentum  $k$  along the tunnelling direction. The angular component of the single particle wave functions in the  $x$ - $y$ -plane perpendicular to the tunnelling direction is quantized in channels  $m \geq 0$ .

Due to the small lateral size of the dot comparable to the magnetic length in the magnetic field range considered ( $B = 10 \dots 30$  T) the Coulomb interaction between the dot and the emitter electron rapidly decreases with  $m$ . The observed FES can then essentially be described by only considering electrons tunnelling from the  $m = 0$  channel through the dot. Using this simplest as-

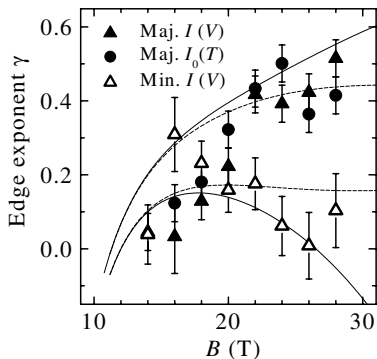


**Fig. 7.** Comparison of the experimentally measured edge exponents  $\gamma$  extracted from temperature dependence (circles) slope fitting (triangles) to the theoretical model (solid and dashed line). The majority spin in the emitter is shown with filled symbols, open symbols correspond to the minority spin. For the solid lines level broadening has been neglected, the dashed curves include an experimentally measured level broadening  $\Gamma = 1.3$  meV [6]

sumption it is already possible to predict a high edge exponent of the order of unity for the FES observed experimentally for high magnetic fields [13].

Following the standard models on FESs [9,16,17,18] we have gone a step further and have developed a full theory which can directly calculate the edge exponent  $\gamma$  for the FES of an electron with spin  $\sigma$  tunnelling from a fully Landau quantized three-dimensional emitter through a small InAs quantum dot [6]. Including all channels  $m$  this model predicts even for a realistic sample with a finite Landau level broadening edge exponents as high as  $\gamma \approx 0.5$ , going far beyond earlier theoretical considerations only valid for  $\gamma \ll 1$  [9].

The resulting theoretically calculated edge exponents  $\gamma$  for both spin orientations are shown in Fig. 7. Already the simple model with no Landau level broadening ( $\Gamma = 0$ , solid lines) describes the experimentally measured edge exponents for both spin directions reasonably well. When a realistic Landau level broadening  $\Gamma = 1.3$  meV is included (dashed lines) the field dependence of the edge exponent is smeared out in high fields and the experimentally measured edge exponents are reproduced even better. The basic features, however, remain unchanged. In particular, the edge exponent for the majority spin still shows a strong field dependence and reaches a very high value  $\gamma \approx 0.5$  at the maximum field  $B = 30$  T. The edge exponent related to the minority spin retains a moderate value  $\gamma \approx 0.15$  for high magnetic fields.

## 5 Conclusion

In conclusion, we have studied the influence of a high magnetic field on resonant tunnelling through individual self-assembled InAs QDs. We have deduced the  $g$ -factor of a single dot from these measurements. We have shown that  $g$  is positive and is systematically increasing with decreasing dot size. Additionally,  $g$  has been shown to feature a pronounced anisotropy with the smallest value when the magnetic field is applied into the direction of strongest confinement. Strongly enhanced current peaks appearing in high magnetic fields have been modelled as a field induced Fermi-edge singularity

originating from the interaction between a localized charge and the electrons in the Landau quantized three-dimensional emitter. Edge exponents as high as  $\gamma = 0.5$  have been both measured experimentally and described theoretically.

## Acknowledgements

We would like to thank U. F. Keyser, A. Nauen J. Regul, and H. W. Schumacher for experimental assistance. The experiments in the Grenoble High Magnetic Field Laboratory were supported by the TMR Programme of the European Union under contract no. ERBFMGECT950077.

## References

1. I. E. Itskevich, T. Ihn, A. Thornton, M. Henini, T. J. Foster, P. Moriarty, A. Nogaret, P. H. Beton, L. Eaves and P. C. Main, Phys. Rev. B **54**, 16401 (1996). [3](#)
2. T. Suzuki, K. Nomoto, K. Taira and I. Hase, Jpn. J. Appl. Phys. **36**, 1917 (1997). [3](#)
3. M. Narihiro, G. Yusa, Y. Nakamura, T. Noda and H. Sakaki, Appl. Phys. Lett. **70**, 105 (1997). [3](#)
4. I. Hapke-Wurst, U. Zeitler, H. W. Schumacher, R. J. Haug, K. Pierz and F. J. Ahlers, Semicond. Sci. Technol. **14**, L41 (1999). [3](#), [4](#), [5](#)
5. A. S. G. Thornton, T. Ihn, P. C. Main, L. Eaves and M. Henini, Appl. Phys. Lett. **73**, 354 (1998). [3](#), [7](#)
6. I. Hapke-Wurst, U. Zeitler, H. Frahm, A. G. M. Jansen, R. J. Haug, and K. Pierz, Phys. Rev. B **62**, 12621 (2001). [3](#), [5](#), [7](#), [10](#), [11](#)
7. J.-M. Meyer, I. Hapke-Wurst, U. Zeitler, R. J. Haug, and K. Pierz, physica status solidi(b) **224**, 685 (2001). [3](#), [8](#)
8. I. Hapke-Wurst, U. Zeitler, R. J. Haug, and K. Pierz, Physica E **12**, 802 (2002). [3](#), [8](#)
9. K. A. Matveev and A. I. Larkin, Phys. Rev. B **46**, 15337 (1992). [4](#), [10](#), [11](#)
10. P. C. Main, A. S. G. Thornton, R. J. A. Hill, S. T. Stoddart, T. Ihn, L. Eaves, K. A. Benedict and M. Henini, Phys. Rev. Lett. **84**, 729 (2000). [6](#)
11. L. M. Roth und P. N. Argyres, in *Semiconductors and Semimetals (Volume 1: Physics of III-V compounds)*, p159 (Academic Press New York London,1966). [7](#)
12. K. Pierz, Z. Ma, I. Hapke-Wurst, U. F. Keyser, U. Zeitler and R. J. Haug, Physica E, in press. [8](#)
13. I. Hapke-Wurst, PhD Thesis, Hannover (2002). [7](#), [8](#), [10](#), [11](#)
14. A. A. Kiselev, E. L. Ivchenko, and U. Rössler, Phys. Rev. B **58**, 16353 (1998). [8](#)
15. A. K. Geim, P. C. Main, N. La Scala, Jr., L. Eaves, T. J. Foster, P. H. Beton, J. W. Sakai, F. W. Sheard, M. Henini, G. Hill and M. A. Pate, Phys. Rev. Lett. **72**, 2061 (1994). [10](#)
16. G. D. Mahan, Phys. Rev. **163**, 612 (1967); G. D. Mahan, *Many-Particle Physics* (Plenum, New York, 1981). [11](#)
17. P. Nozières and C. T. De Dominicis, Phys. Rev. **178**, 1097 (1969). [11](#)
18. K. D. Schotte and U. Schotte, Phys. Rev. **182**, 479 (1969). [11](#)